

Supporting Information

MoS₂/CoS heterostructures grown on carbon cloth as free-standing anodes for high-performance sodium-ion batteries

Fangfang Xue^a, Feifan Fan^a, Zhicheng Zhu^a, Zhigang Zhang^a, Yuefeng Gu^b, QiuHong Li^{a,b,*}

^a*Pen-Tung Sah Institute of Micro-Nano Science and Technology, Xiamen University, Xiamen 361005, China. E-mail: liqiuHong@xmu.edu.cn; Fax: +86-0592-2187196; Tel: +86-0592-2187198*

^b*School of Electronic Science and Engineering, Xiamen University, Xiamen 361005, China*

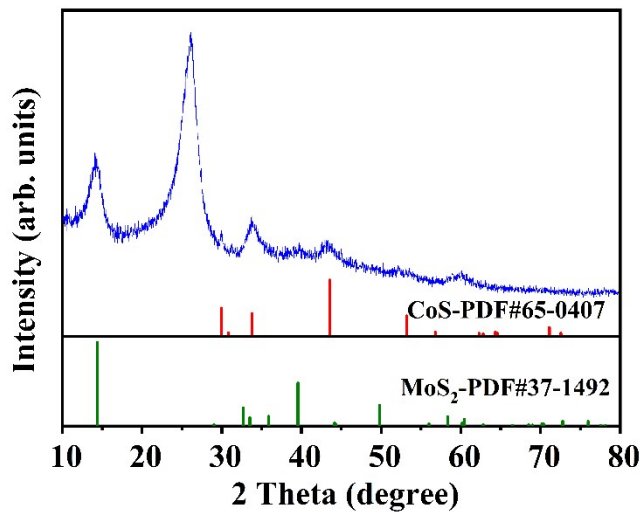


Fig. S1 The XRD pattern of MoS₂/CoS@CC intermediate.

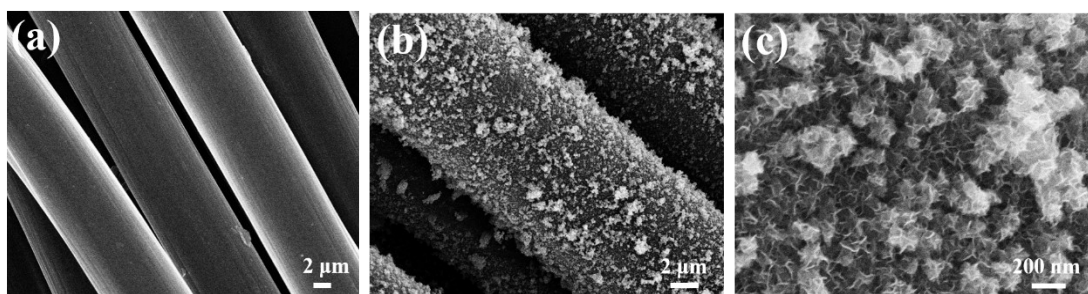


Fig. S2 SEM images of bare CC (a) and MoS₂/CoS intermediate arrays on CC (b, c), respectively.

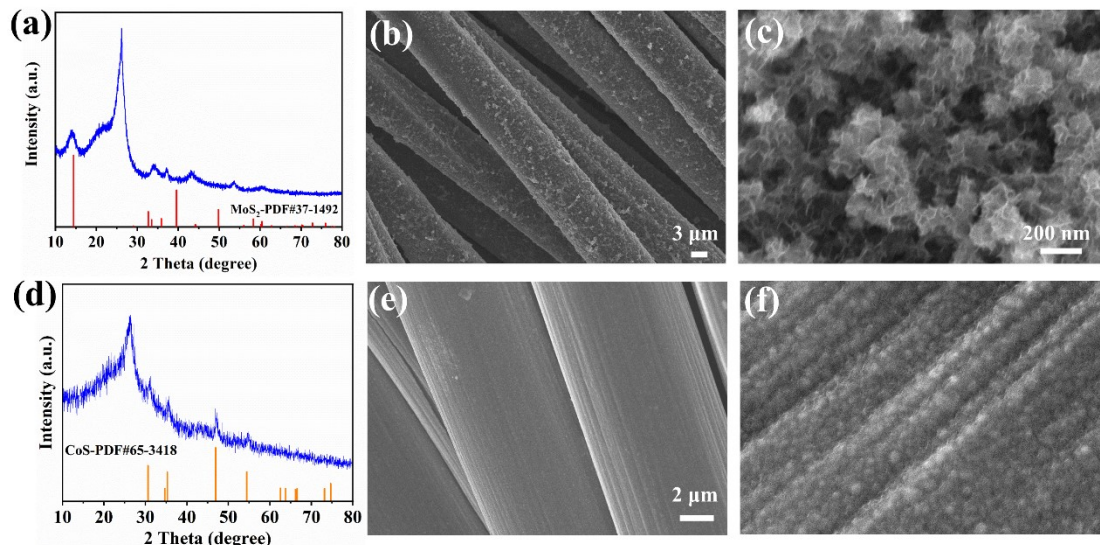


Fig. S3 (a) XRD pattern, and (b,c) SEM images of MoS₂@CC; (d) XRD pattern, and (e,f) SEM images of CoS@CC.

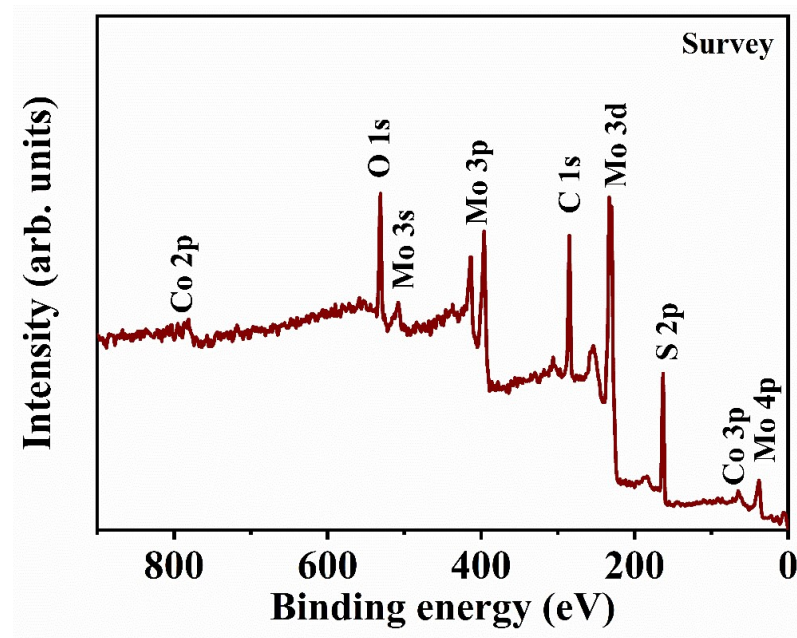


Fig.S4 XPS survey spectrum of $\text{MoS}_2/\text{CoS}@\text{CC}$.

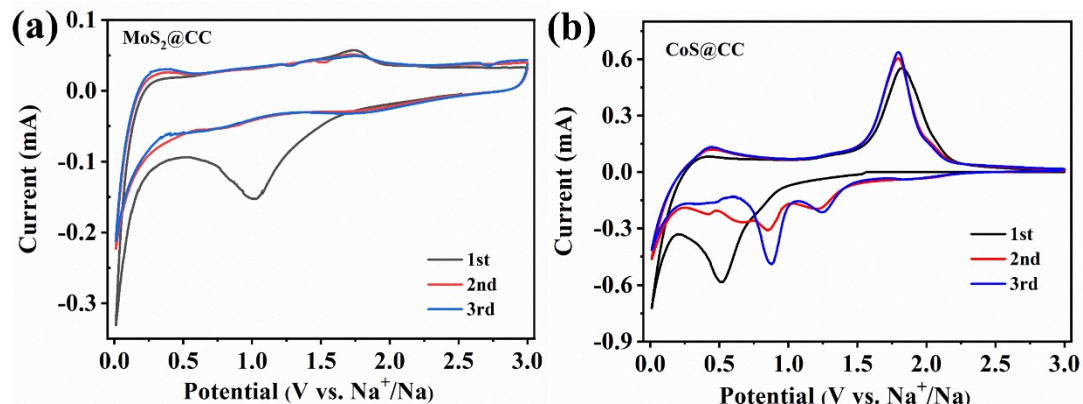


Fig.S5 CV curves of $\text{MoS}_2@\text{CC}$ (a) and $\text{CoS}@\text{CC}$ (b) at a scan rate of 0.1 mV s^{-1} .

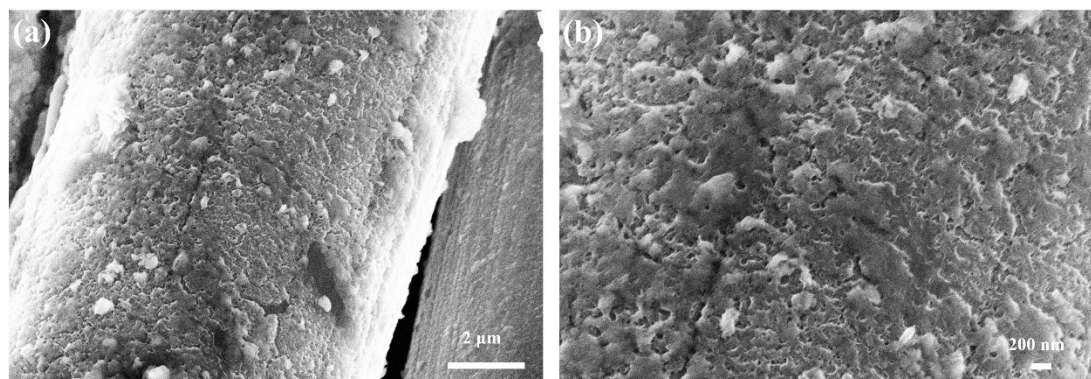


Fig.S6 SEM images of $\text{MoS}_2/\text{CoS}@\text{CC}$ electrodes after 100 cycles at a current density of 0.5 A g^{-1} .

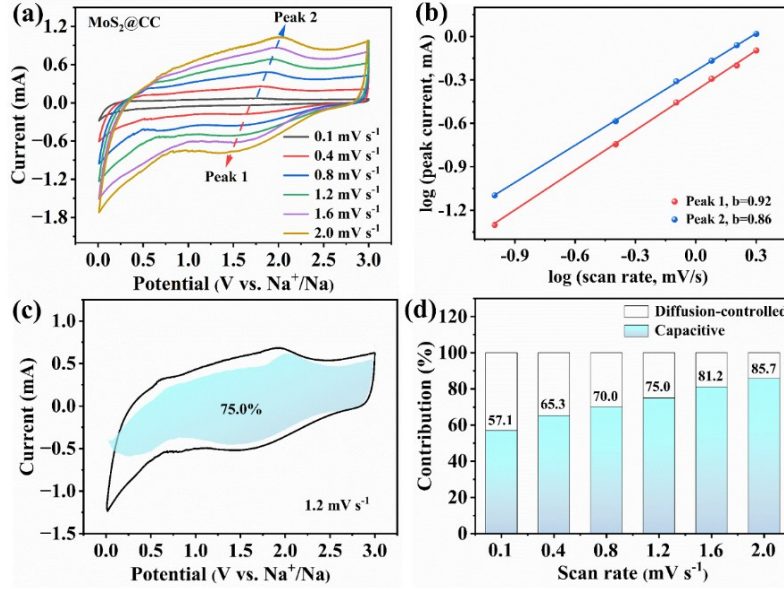


Fig.S7 (a) CV curves of plain $\text{MoS}_2@\text{CC}$ electrode at different scan rates. (b) The corresponding relationship between $\log(i)$ vs. $\log(v)$ at each redox peak current. (c) CV curve of the capacitive-controlled capacity at 1.2 mV s^{-1} , denoted by the shaded area. (d) The capacitive- and diffusion-controlled behavior contribution ratios at different scan rates.

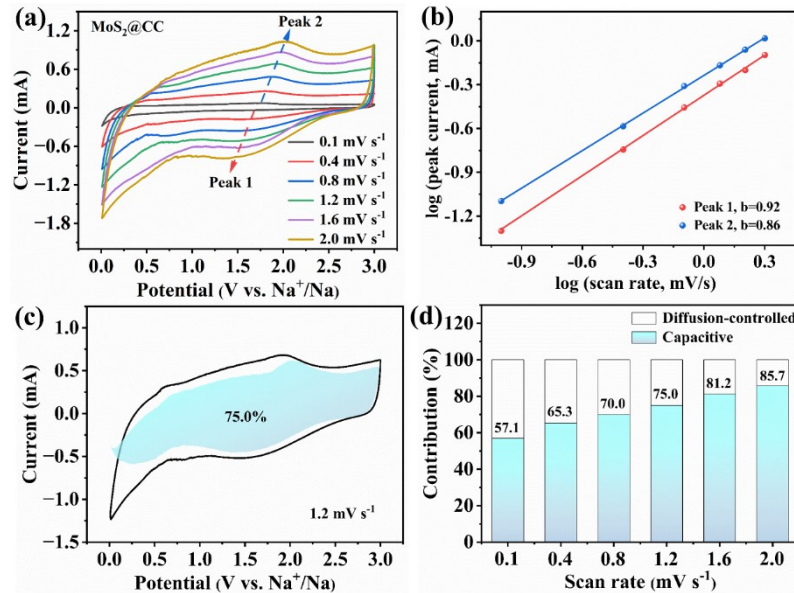


Fig.S8 (a) CV curves of plain $\text{CoS}@\text{CC}$ electrode at different scan rates. (b) The corresponding relationship between $\log(i)$ vs. $\log(v)$ at each redox peak current. (c) CV curve of the capacitive-controlled capacity at 1.2 mV s^{-1} , denoted by the shaded area. (d) The capacitive- and diffusion-controlled behavior contribution ratios at different scan rates.

Table S1 Electrochemical performances of reported MoS₂-based anode for SIBs.

Materials	Cyclability (mAh g ⁻¹)	Rate capability (mAh g ⁻¹)	Ref
1T MoS ₂ nanosheets	410 at 0.1 A g ⁻¹ after 150 cycles	253 at 2.0 A g ⁻¹	[1]
MoS ₂ -CNF	525 at 0.05 A g ⁻¹ after 70 cycles	186 at 2.0 A g ⁻¹	[2]
HMF-MoS ₂	384 at 0.1 A g ⁻¹ after 100 cycles	226 at 5.0 A g ⁻¹	[3]
NiS/MoS ₂ /C	516 at 0.1 A g ⁻¹ after 60 cycles	398 at 5.0 A g ⁻¹	[4]
MoS ₂ -graphene	313 at 0.05 A g ⁻¹ after 200 cycles	175 at 2.0 A g ⁻¹	[5]
MoS ₂ /CoS ₂	396.6 at 0.1 A g ⁻¹ after 80 cycles	389 at 0.5 A g ⁻¹	[6]
MoS ₂ @CF	100 at 0.1 A g ⁻¹ after 100 cycles	171 at 5.0 A g ⁻¹	[7]
Cu ₂ S@carbon@MoS ₂	365 at 0.3 A g ⁻¹ after 100 cycles	297 at 3.0 A g ⁻¹	[8]
MoS₂/CoS@CC	605 at 0.5 A g⁻¹ after 100 cycles	366 at 8.0 A g⁻¹	This work

Table S2 Fitting results of Nyquist plots based on the equivalent circuit in Fig. 5e.

Electrodes	R _{ct}	R _s	σ (Ω cm ² s ^{-1/2})
MoS ₂ /CoS@CC	155.2	6.0	548.0
MoS ₂ @CC	466.9	7.0	1363.3
CoS@CC	204.1	3.2	824.6

References

- [1] D. Sun, D. Huang, H.Y. Wang, G.L. Xu, X.Y. Zhang, R. Zhang, Y.G. Tang, D. Abd Ei-Hady, W. Alshitari, A.S. Al-Bogami, K. Amine and M.H. Shao, *Nano Energy*, 2019, **61**, 361-369.
- [2] Q. Ni, Y. Bai, S.N. Guo, H.X. Ren, G.H. Chen, Z.H. Wang, F. Wu and C. Wu, *ACS Appl. Mater. Interfaces*, 2019, **11**, 5183-5192.
- [3] Y. Li, R.P. Zhang, W. Zhou, X. Wu, H.B. Zhang, J. Zhang, *ACS Nano*, 2019, **13**, 5533-5540.
- [4] H.Q. Xie, M. Chen and L.M. Wu, *ACS Appl. Mater. Interfaces*, 2019, **11**, 41222-41228.
- [5] X. Geng, Y. Jiao, Y. Han, A. Mukhopadhyay, L. Yang and H. Zhu, *Adv. Funct. Mater.*, 2017, **27**, 1702998.
- [6] Y. Su, C.X. Wu, H. Li, F.J. Chen, Y. Guo, L. Yang and S.L. Xu, *J. Alloys Compd.*, 2020, **845**, 156229.
- [7] Z.H. Zhao, X.D. Hu, H.Q. Wang, M.Y. Ye, Z.Y. Sang, H.M. Ji, X.L. Li and Y.J. Dai, *Nano Energy*, 2018, **48**, 526–535.
- [8] Y.J. Fang, D.Y. Luan, Y. Chen, S.Y. Gao and X.W. Lou (David), *Angew. Chem. Int. Ed.*, 2020, **59**, 7178 –7183.